Electromagnetic Design of a Magnetic Suspension System

William G. Hurley, *Senior Member, IEEE*, and Werner H. Wölfle

Abstract— Magnetic levitation of a metallic sphere provides a high-impact visual demonstration of many principles in undergraduate educational programs in electrical engineering, e.g., electromagnetic design, compensation of a unstable control system, and power amplifier design. This paper deals with the electromagnetic and dynamic analysis of the levitation system and it has design formulas which are derived from first principles. This analysis leads to a plant transfer function which is used to implement a proportional plus derivative (PD) compensation strategy. Issues covered include coil and wire sizing for a given temperature rise. The paper shows that the electromagnet can be optimized for a given sphere. An experimental system is described which levitates a 6-cm, 0.8-kg sphere.

Index Terms— Compensation, control engineering education, electromagnets, magnetic levitation, proportional control.

INDEX OF SYMBOLS

A_c	Area of core cross section.
A_p	Product of window area (W_A) and area of core (A_c).
A_t	Surface area of electromagnet.
A_w	Bare copper area.
a	See (1) and Fig. 2.
D	Diameter of suspended sphere.
d	Airgap distance at equilibrium position.
G	Output current/position gain (A/m), (32).
G_F	Power amplifier transconductance (A/V), (32) and (40).
G_s	Sensor gain (V/m), (31).
g	Acceleration due to gravity, 9.81 m/s^2.
g_{fs}	Transconducatance of FET.
h	Height of coil window.
h_c	Heat-transfer coefficient.
I	Equilibrium current in the coil.
J	Current density.
K_p	Proportional gain.
K_t	See (17).
K_u	Window utilization factor.
$L(x)$	Inductance at position x.
L_1	Inductance at $x = \infty$.
L_0	Incremental inductance due to sphere at $x = 0$.
L_d	Incremental inductance per turn at equilibrium position.
ℓ_t	Mean length of a turn.

M	Mass of sphere.
N	Number of turns.
t	Jacket thickness.
T_d	Derivative time.
W_A	Window area.
W_m	Stored energy in electromagnet.
w	Width of coil window.
x	Airgap distance.
Δ	Core diameter.
ΔT	Temperature rise in the electromagnet.
ρ	Electrical resistivity of the coil conductor.
μ_0	Permeability of free space $4\pi \times 10^{-7}$ H/m.
$\omega_n = \sqrt{\frac{g}{a}}$	Natural frequency (r/s).

I. INTRODUCTION

THE stable suspension of a metallic sphere in a magnetic field has been a subject of considerable interest since the 1930's. Aside from its visual impact it serves to illustrate many fundamental principles of electrical and electronic engineering: electromagnetism and electrodynamics [1], control theory [2], and analog [3] and digital [4], [5] circuit design. In particular the application of PD control and lead control have been extensively reported for both analog and digital controllers [1]–[5]. The design and implementation of the magnetic system has been largely ignored. The purpose of this paper is to address this deficiency. The system is designed to successfully levitate a 6-cm-diameter steel ball with a mass of 0.8 kg, which is significantly larger than anything already reported. A set of design rules is presented which enables the reader to design an optimum magnet for a given size ball. Coil dimensions and wire sizing for a given temperature rise are treated in detail. For completeness, the full circuit of a working model is described. All the equations are derived from first principles in order to emphasize the value of the system as an educational tool.

II. ELECTROMAGNETIC SYSTEM

The principal components of the magnetic suspension system are shown in Fig. 1. The position of the ball is sensed by the optical system and the feedback signal is used to control the position of the steel ball.

The inductance of the coil varies with ball position as illustrated in Fig. 2. The essential features are: L_1 is the inductance when the ball is removed ($x = \infty$), $L_0 + L_1$ is the inductance when the ball is in contact with the coil ($x = 0$). The variation in inductance between these two extremes can be
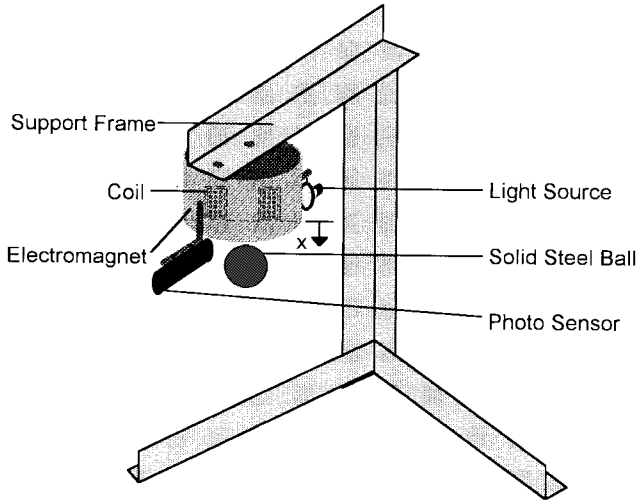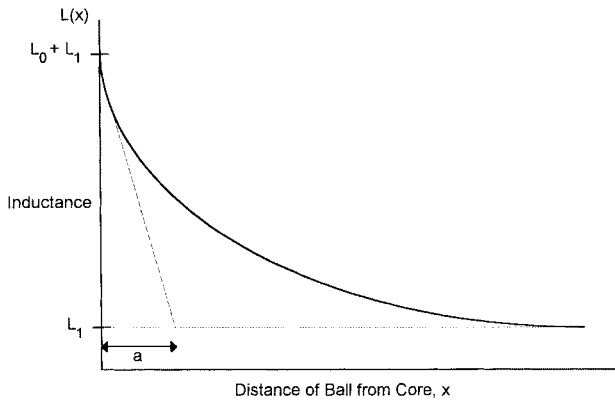
Fig. 1. The electromagnetic suspension system.

Fig. 2. The coil inductance as a function of separation.

described in many different ways; for mathematical simplicity, it is sufficiently accurate to use an exponential function

$$L(x) = L_1 + L_0 e^{-x/a} \qquad (1)$$

where "a" is the length constant. The magnetic co-energy of the system is a function of coil current i and separation x

$$W'(i,x) = \tfrac{1}{2} L(x) i^2. \qquad (2)$$

The force of magnetic origin acting on the ball is given by

$$f = \frac{\partial W'}{\partial x} = -\frac{L_0}{2a} i^2 e^{-x/a}. \qquad (3)$$
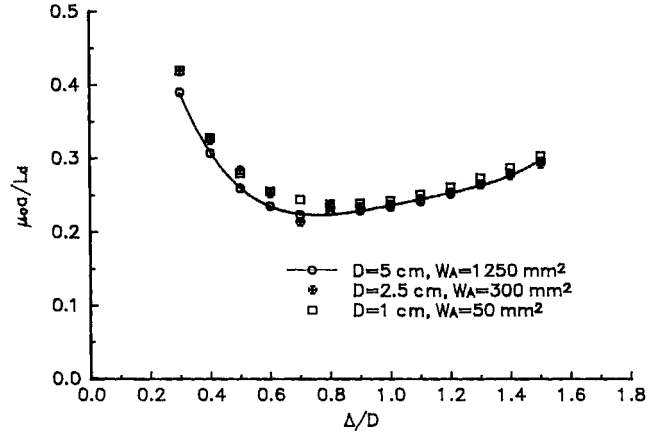
In static equilibrium this force is exactly balanced by the gravitational force acting on the ball. At $x = d$, $i = I$

$$Mg = \frac{L_0}{2a} e^{-d/a} I^2 = \frac{N^2 L_d}{2a} I^2 \qquad (4)$$

where N is the number of turns in the coil, L_d is the incremental inductance at $x = d$ due to a single-turn coil, and $g = 9.81$ m/s^2 is the acceleration due to gravity.

Rearranging (4) gives

$$I = \sqrt{2Mg\frac{a}{N^2 L_d}}. \qquad (5)$$

Fig. 3. Optimizing the core diameter, $d = 0.2D$.

Evidently, the ratio $\frac{a}{L_d}$ is required in order to predict the steady-state coil current. Furthermore, this quantity can be optimized to minimize the coil current. This is the subject of the next section.

III. OPTIMIZED DESIGN OF THE ELECTROMAGNET

Equation (5) shows that it is the incremental inductance due to the presence of the ball which determines the steady-state coil current. The magnetic system of Fig. 1 was simulated using Finite Element Analysis [6]. The first step in optimizing the design is to investigate the core diameter. The dimensionless parameter $\mu_0 \frac{a}{L_d}$ is plotted in Fig. 3 for the ratio Δ/D, where Δ is the core diameter and D is the ball diameter for three values of D: 5 cm, 2.5 cm, and 1 cm, respectively. In this figure, the equilibrium separation is $d = 0.2D$, the window width is $w = D/2$, the window height is $h = 2w$, and the jacket thickness is $t = 0.2D$. The graph clearly establishes that $\Delta/D = 0.8$ is the optimum core dimension. The winding area is chosen for 1000 turns of wire which is selected for the appropriate current given by (5). The current density and, consequently, the wire size are determined by the thermal design, which is addressed in the next section.

The ratio $\frac{h}{w}$ was investigated for a constant window area and it was found that the design parameter $\mu_0 \frac{a}{L_d}$ remained constant for $\frac{h}{w}$ in the range 1.5–5.0. For aesthetic reasons, the value $\frac{h}{w} = 2.0$ is chosen and the overall height is approximately equal to one half of the overall diameter. The thickness of the outer jacket was investigated and it was found that it should be at least 10% of D, thus ensuring that the reluctance of the return path is at least as low as the reluctance of the cylindrical core. For the 5-cm ball $\mu_0 \frac{a}{L_d} = 0.228$, one of the remarkable features of Fig. 3 is that this parameter is nearly constant for all values of D at the optimum point. If the outer jacket in Fig. 1 is removed this value becomes 0.882, which would increase the coil current by a factor of 2.0 for the same number of turns, as shown by (5).

Fig. 4 shows the optimum value of core diameter versus ball position. As the separation increases, the optimum core diameter also increases. As the gap increases more flux returns from the core to the outer jacket in the airgap. The coupling
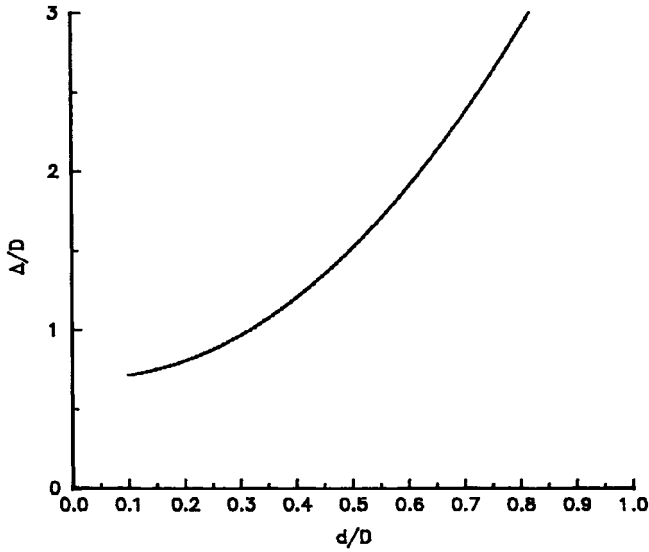
Fig. 4. Optimum core diameter versus separation, $D = 5$ cm.

TABLE I
OPTIMIZED CORE PARAMETERS ($N = 1000, d = 0.2\,D$)

D (cm)	L_0 (H)	L_1 (H)	a (mm)	$\mu_0 \frac{a}{L\,d}$
5.0	0.191	0.291	5.35	0.228
2.5	0.093	0.143	2.68	0.234
1.0	0.036	0.056	1.08	0.238

to the ball is reduced and the length constant "a" is increased. The finite-element analysis has shown that the length constant "a" is approximately given by $a = D/9$. By analogy with the classical concept of "time constant" in an RC circuit we would expect that the effective operating range for ball separation would be up to $4a$ or 45% of the ball diameter. This is confirmed in Fig. 4 where the core diameter increases exponentially for $d/D > 0.45$ and the physical size of the electromagnet would be impractical to build.

Table I is a summary of the principal parameters in Fig. 3.

IV. DESIGN OF THE ELECTROMAGNET

The energy stored in the coil at equilibrium is

$$W_m = \tfrac{1}{2} L(d)I^2 = \tfrac{1}{2} B_m A_c N I \qquad (6)$$

where B_m is the flux density in the core and A_c is the core cross-sectional area. This assumes that in the absence of leakage flux the same flux links the N-turn winding N times and also that the flux density is constant over the cross section.

The window utilization factor K_u in the amount of copper in the window area W_A

$$K_u = \frac{NA_w}{W_A} \qquad (7)$$

where A_w is the bare copper area of the wire. The current density is
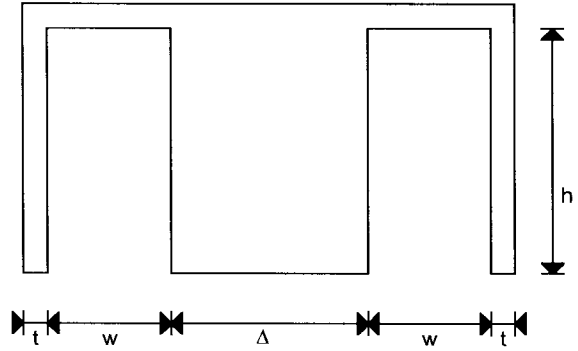
$$J = \frac{I}{A_w}. \qquad (8)$$

Fig. 5. Optimum coil dimensions.

The copper losses are given by

$$P_{\text{cu}} = RI^2 = R(JA_w)^2. \qquad (9)$$

The dc resistance of the coil is

$$R = \frac{\rho N \ell_t}{A_w} \qquad (10)$$

where ρ is the resistivity of copper ($1.72 \times 10^{-8}\,\Omega \cdot \text{m}$) and ℓ_t is the mean length of a coil turn.

The heat loss by natural convection from the surface of the coil is

$$P = h_c A_t \Delta T \qquad (11)$$

where h is the heat transfer coefficient (10 W/m^2 $\cdot$ °C), A_t is the surface area of the coil, and ΔT is the temperature rise in the coil. It is assumed that conduction of heat through the copper and steel does not make a significant contribution to temperature rise.

Substituting (10) into (9) and equating with (11) gives

$$J = \sqrt{\frac{h_c A_t \Delta T}{\rho \ell_t N A_w}}. \qquad (12)$$

A useful measure of the coil size is the product of the window area and the core cross-sectional area

$$A_p = W_A A_c. \qquad (13)$$

In the optimum coil design:

core diameter $\Delta = 0.8D$
window width $w = 0.5D$
window height $h = 2w$
jacket thickness $t = 0.1D$.

These dimensions are illustrated in Fig. 5.

The physical quantities W_A, A_t, and ℓ_t may be related to the core parameter A_p by dimensional analysis

$$W_A = \sqrt{A_p} \qquad (14)$$
$$A_t = 26\sqrt{A_p} \qquad (15)$$
$$\ell_t = 6\sqrt[4]{A_p}. \qquad (16)$$

Substituting (7), (14), (15), and (16) into (12) with $K_u = 0.6$ yields

$$J = K_t \frac{\sqrt{\Delta T}}{\sqrt[8]{A_p}} \qquad (17)$$

where $K_t = 64.8 \times 10^3$ A/m$^{3/2} \cdot {}^\circ$C$^{1/2}$ for J in A/m^2 with ΔT in $^\circ$C and A_p in m^4. Combining (6)–(8)

$$W_m = \tfrac{1}{2}B_m A_c J K_u W_A. \tag{18}$$

Substituting (13) and (17) in (18) after rearranging

$$A_p = \left[\frac{2W_m}{B_m K_u K_t \sqrt{\Delta T}}\right]^{8/7}. \tag{19}$$

Rewriting (6) with I given by (5) and substituting into (19), gives A_p in terms of

$$A_p = \left[\frac{A_c\sqrt{2Mg\frac{a}{L_d}}}{K_u K_t \sqrt{\Delta T}}\right]^{8/7}. \tag{20}$$

Equation (20) sizes the core for a particular sphere and temperature rise.

Equation (20) can be further simplified by noting the optimum conditions of Fig. 3: $\mu_0 \frac{a}{L_d} = 0.228$ and $\Delta = 0.8D$. Furthermore, $g = 9.81$ m/s^2 and for $K_u = 0.6$, $K_t = 64.8 \times 10^3$ A/m$^{3/2} \cdot {}^\circ$C$^{1/2}$ and $\Delta T = 30^\circ$C

$$A_p = 0.002M^{4/7}D^{16/7}. \tag{21}$$

For example, $M = 0.8$ kg, $D = 0.06$ m, $A_p = 284 \times 10^{-8}$ m^4. Taking the density of steel as 7100 kg/m^3 for a steel sphere (21) further simplifies to

$$A_p = 0.22D^4. \tag{22}$$

A. Selecting the Number of Turns

The number of turns in the electromagnet influences the following three design issues:
- copper losses
- flux density in the core
- dc operating point of the power amplifier.

1) Copper Losses: The copper or winding losses are given by (9) and combining with (5), (7), and (10)

$$P_{\text{cu}} = \frac{\rho \ell_t 2Mg}{K_u W_A}\frac{a}{L_d}. \tag{23}$$

Evidently, the copper losses are independent of the number of turns. The coil current can be reduced by increasing the number of turns but this is offset by the increased resistance of a smaller wire. The window area remains essentially constant in (23) because the increase in the number of turns in offset by the smaller cross-sectional area of the wire. Larger wire may be used to reduce the losses at the expense of a bigger electromagnet.

2) Flux Density: The flux density in the core of the electromagnet is determined by the MMF (NI) of the coil. Examination of (5) shows that the product NI is fixed by the mass of the sphere and the optimized parameter $\mu_0 \frac{a}{L_d}$.

3) Amplifier Operating Point: The loadline of the power amplifier is determined by the power supply voltage and the coil resistance. The voltage drop in the coil is RI and (5), (7), and (10) show that this product is increased if the current is reduced by incorporating a greater number of turns in the electromagnet. The voltage drop in the coil can be reduced by using a larger wire at the expense of a larger electromagnet.
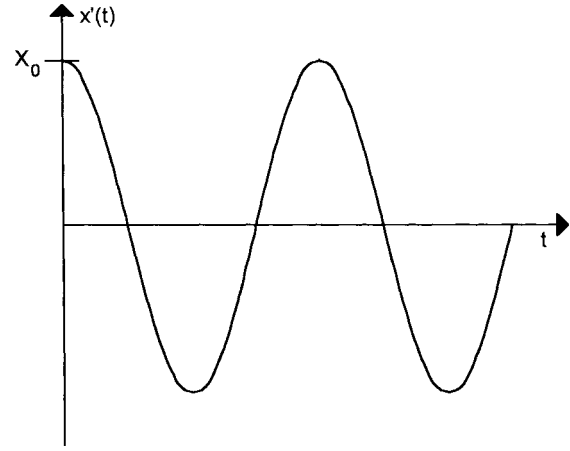

Fig. 6. Dynamic response for $G > \frac{I}{2a}$.

V. THE DYNAMIC SYSTEM

The force of magnetic origin, acting on the ball is given by (3)

$$f(i,x) = -\frac{1}{2a}L_0 e^{-x/a}i^2. \tag{24}$$

Consider a perturbation about the equilibrium at $x = d$, $i = I$

$$x = d + x'$$
$$i = I + i'$$
$$f = f + f'.$$

By Taylor's series expansion

$$f(i,x) = f(I,d) + \left.\frac{\partial f}{\partial x}\right|_{I,d} x' + \left.\frac{\partial f}{\partial i}\right|_{I,d} i'. \tag{25}$$

From (24)

$$f' = \frac{1}{2a^2}L_0 e^{-d/a}I^2 x' - \frac{I}{a}L_0 e^{-d/a}Ii'. \tag{26}$$

The mechanical force is

$$f^m = Mg + M\frac{d^2x'}{dt^2}.$$

At equilibrium, $Mg = f(I,d)$ given by (4), and the incremental equation of motion becomes

$$M\frac{d^2x'}{dt^2} - \frac{N^2 L_d I^2}{2a^2}x' + \frac{N^2 L_d I}{a}i' = 0. \tag{27}$$

Taking Laplace transforms

$$\frac{X(s)}{I(s)} = -\frac{\dfrac{N^2 L_d I}{a}}{Ms^2 - \dfrac{N^2 L_d I^2}{2a^2}}. \tag{28}$$

Using (5)

$$\frac{X(s)}{I(s)} = \frac{-\frac{2g}{I}}{s^2 - \omega_n^2} \tag{29}$$

$$\omega_n = \sqrt{g/a}. \tag{30}$$

This is the plant transfer function which relates the coil current and ball position. The position of the ball is sensed optically, and a voltage is produced which is proportional to the ball position

$$v_s' = G_s x' \tag{31}$$

where G_s is the sensor gain (V/m).

This voltage is applied to the gate of a field-effect transistor (FET) amplifier which has the coil in the drain circuit

$$i' = G_F v_s' = G_F G_s x' = G x' \tag{32}$$

where G_F is the transconductance of the power amplifier.

Substituting for i' given by (32) into (27) yields

$$M\frac{d^2 x'}{dt^2} + \frac{N^2 L_d I}{a}\left[G - \frac{I}{2a}\right]x' = 0. \tag{33}$$

This is a second-order differential equation. The characteristic equation in (33) is

$$\lambda^2 + \omega_n'^2 = 0 \tag{34}$$

$$\omega_n' = \sqrt{\frac{N^2 L_d I}{Ma}\left[G - \frac{I}{2a}\right]} \tag{35}$$

ω_n' is either real or complex depending on the quantity $[G - \frac{I}{2a}]$. For $G > \frac{I}{2a}$, ω_n' is real and the solution of (33) is of the form

$$x'(t) = A\cos\omega_n' t + B\sin\omega_n' t \tag{36}$$

where A and B are determined by initial conditions. $x'(t)$ is a pure sinusoid.

For $x'(0) = X_0$ and $\frac{dx'}{dt} = 0$ at $t = 0$ the solution is illustrated in Fig. 6. For $G < \frac{I}{2a}$, ω_n' is complex and the solution of (33) is a growing exponential which is not suitable for the suspension system.

VI. CONTROL

The sustained oscillation described in Fig. 6 can only be achieved by a perfect current source. A block diagram of the control system is shown in Fig. 7 along with its associated root locus plot.

The poles on the imaginary axis are given by $G > \frac{I}{2a}$ as shown in Section V.

A damping term could be introduced into (33) by means of a lead transfer function of the form [7]

$$\frac{V_2}{V_1} = \frac{1}{\alpha}\frac{\alpha\tau s + 1}{\tau s + 1}. \tag{37}$$

For $\alpha \gg 1$, the transfer function between the zero and the pole is approximately

$$\frac{V_2}{V_1} = \frac{1}{\alpha}(\alpha\tau s + 1). \tag{38}$$

This is the classical form of PD control, which may be written

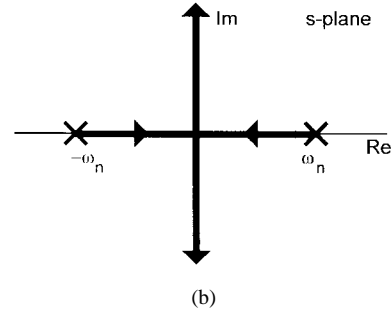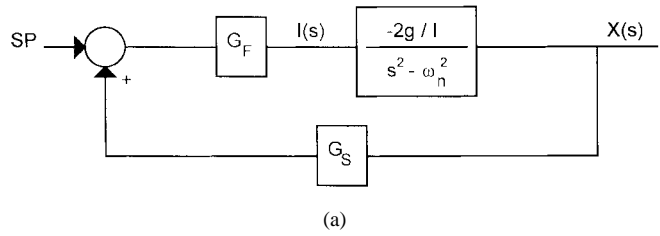$$\frac{V_2}{V_1} = K_p(1 + T_d s). \tag{39}$$

Fig. 7. (a) Black diagram and (b) root locus of uncompensated system.
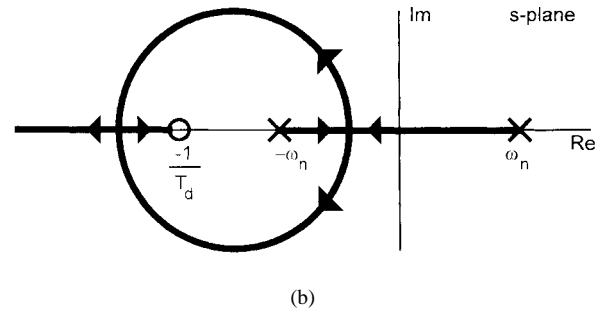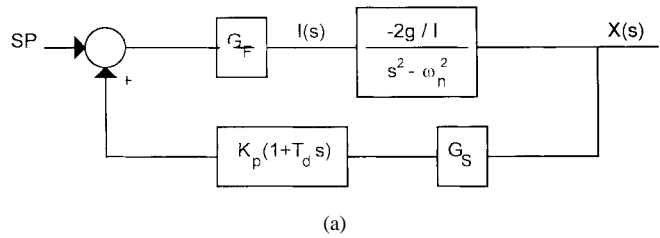

Fig. 8. (a) Block diagram and (b) root locus of compensated system.

If $v_1(t)$ is the output of the position sensor then $v_2(t)$ has a component which is proportional to the velocity of the ball.

The block diagram with PD control and its associated root locus is shown in Fig. 8. The value of K_p may be chosen for a suitable value of damping ratio and natural frequency.

VII. EXPERIMENTAL SYSTEM

A. The Electromagnet

The analysis of the previous sections was applied to the design of an electromagnetic system with

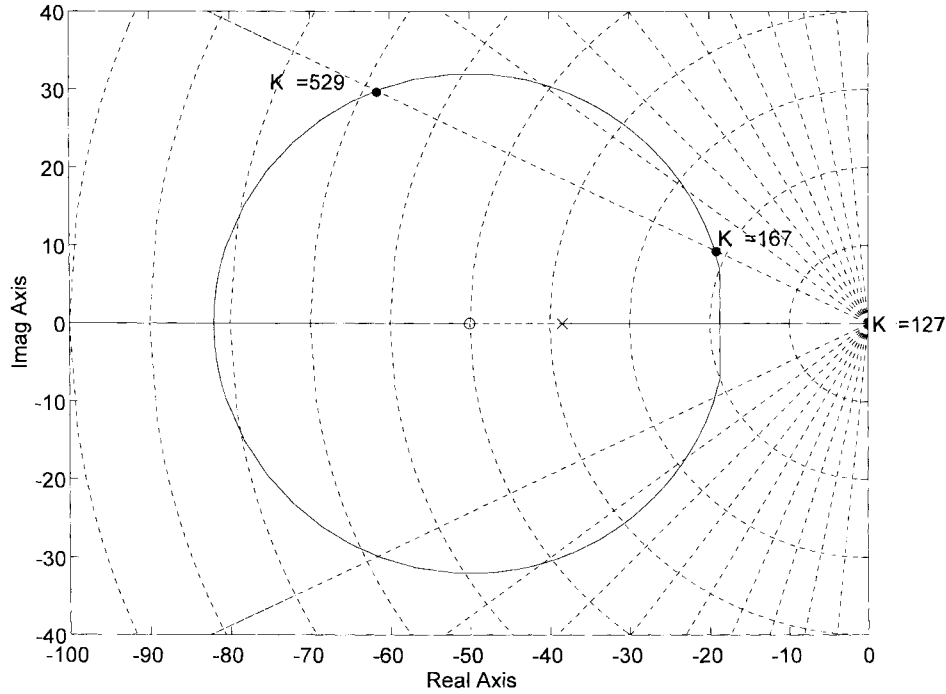|	
mass of sphere	$M = 0.8$ kg
diameter of sphere	$D = 6.0$ cm
equilibrium gap	$d = 1$ cm

Fig. 9. Root locus of the experimental system, loci of damping ratios in increments of 0.1, and loci of natural frequencies in increments of 10 r/s.

Calculations:
Table I:

$$\mu_0 \frac{a}{L_d} = 0.228$$
$$a \cong D/9 = 6.66 \text{ mm}$$

Equation (5), $N = 1000$ turns, $I = 1.69$ A

$$\Delta T = 30°\text{C}, \ \Delta = 0.8D, \ K_u = 0.6,$$
$$K_t = 64.8 \times 10^3 \text{ A/m}^{3/2} \cdot °\text{C}^{1/2}$$

Equation (20)	$A_p = 291$ cm^4	
Equation (17)	$J = 175$ A/cm^2	
Equation (8)	$A_w = 0.971$ mm^2.	

This is a 1.12–mm-diameter wire, resulting in a coil resistance of 4.3 Ω. Extrapolating from Table I, $L_0 = 0.229$ H and $L_1 = 0.349$ H giving $L(d) = 0.4$ H at $d = 1$ cm and the time constant of the coil is 93 ms.

Core dimensions, see Fig. 5

core diameter	$\Delta = 0.8D$	$= 48$ mm
window width	$w = 0.5D$	$= 30$ mm
window height	$h = 2w$	$= 60$ mm
wall thickness	$t = 0.1D$	$= 6$ mm
outside diameter		$= 120$ mm
overall height		$= 66$ mm.

B. Control System

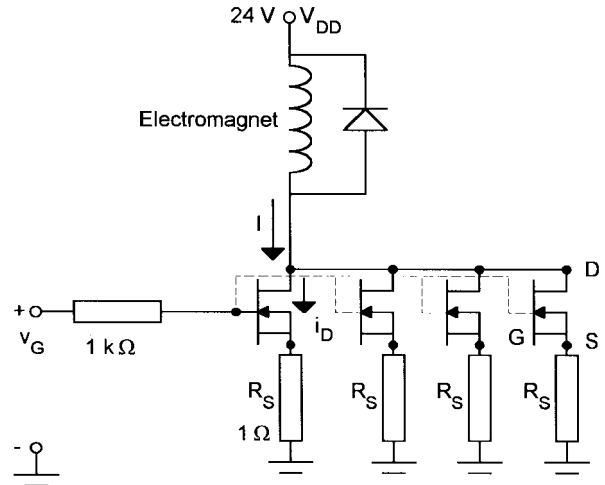|		
sensor gain	G_s	$= 46$ V/m
FET amplifier	G_F	$= 3.2$ A/V
natural frequency	ω_n	$= 38.38$ r/s
derivative time	T_d	$= 20$ ms
proportional gain	K_p	$= 3.6.$

Fig. 10. The power amplifier.

The gain $(G_s K_p G_F)$ is 529 which is shown in the root locus diagram of Fig. 9 and represents a phase margin of 67°. The overall gain is chosen for a maximum gap of 2.0 cm which corresponds to a current of 4.3 A and $G > 323$.

C. The Power Amplifier

The power amplifier is shown in Fig. 10. The coil is placed in the drain circuit. R_s is included for bias stability. The transconductance of the amplifier is given by [8]

$$G_F = \frac{\partial i_D}{\partial v_G} = \frac{g_{fs}}{g_{fs} R_s + 1} \tag{40}$$

where g_{fs} is the transconductance of the power metal–oxide–semiconductor field-effect transistor (MOSFET). For

Fig. 11.   The experimental system.

In educational terms, several issues are addressed: magnetic design, control using root locus and pole placement techniques, power amplifier design, and sensor implementation. Future experiments could include digital control, fuzzy logic control, and a PWM switching power circuit.

REFERENCES

[1] H. H. Woodson and J. R. Melcher, *Electromechanical Dynamics*, pt. 1. New York: Wiley, 1968, ch. 5.
[2] J. K. Roberge, *Operational Amplifiers: Theory and Practice*. New York: Wiley, 1975, ch. 6.
[3] T. H. Wong, "Design of a magnetic levitation control system—An undergraduate project," *IEEE Trans. Educ.*, vol. E-29, pp. 196–200, Nov. 1986.
[4] A. T. Carmichael, S. Hinchliffe, P. N. Murgatroyd, and I. D. Williams, "Magnetic suspension systems with digital controllers," *Rev. Sci. Instrum.*, vol. 57, no. 8, pp. 1611–1615, Aug. 1986.
[5] K. Oguchi and Y. Tomigashi, "Digital control for a magnetic suspension system as an undergraduate project," *Int. J. Elec. Eng. Educ.*, vol. 27, no. 3, pp. 226–236, July 1990.
[6] *User's Manual*, Ansoft Corporation, Maxwell 2D Field Simulator, ver. 4.33, Sept. 1991.
[7] K. Ogata, *Modern Control Engineering*, 2nd ed. Englewood Cliffs, NJ: Prentice Hall, 1990, ch. 7, probl. A-7-5.
[8] J. Millman, *Microelectronics: Digital and Analog Circuits and Systems*. New York: McGraw-Hill, 1979, ch. 11.

$I_D = 1.7$ A, $g_{fs} = 4.0$ Ω^{-1} for BUZ350, according to the manufacturer's data sheet. Thus $G_F = 0.8$ A/V. Four devices are connected in parallel in order to spread the current giving an overall gain of 3.2 A/V.

The constructed system is shown in Fig. 11. The current drawn at $d = 1$ cm is 1.7 A as predicted.

VIII. CONCLUSION

A new set of formulas has been established for the design of an electromagnetic levitation system with a metallic sphere. The design formulas have been derived from first principles and are therefore suitable for other applications. As such they are a useful vehicle to teach the design of magnetic components to undergraduate students.

An unstable second-order plant transfer function is obtained from the design formulas. *A priori* knowledge of the plant transfer function obviates the need to measure the plant parameters after it has been built. It also means that the control system can be designed on paper which eliminates the trial-and-error approach which was necessary in the past. The student can design a compensation system on paper and "see" the results.

William G. Hurley (M'77–SM'90) was born in Cork, Ireland. He graduated from the National University of Ireland, Cork, in 1974 with a 1st class honors Batchelors degree in electrical engineering. He completed the Master's degree in electrical engineering at the Massachusetts Institute of Technology, Cambridge, MA, in 1976, and the Ph.D. degree on transformer modeling at the National University of Ireland, Galway, in 1988.

He worked for Honeywell Controls in Canada as a product engineer from 1977 to 1979 and as a development engineer in transmission lines at Ontario Hydro from 1979 to 1983. He lectured in electronic engineering at the University of Limerick, Ireland, from 1983 to 1991 and is currently a Senior Lecturer in the Department of Electronic Engineering at University College, Galway, Ireland. He is the Director of the Power Electronics Research Center there. His research interests include high-frequency magnetics and power quality.

Dr. Hurley is a member of the Administrative Committee of the Power Electronics Society of the IEEE and a member of Sigma Xi.

Werner H. Wölfle was born in Bad Schussenried, Germany. He received the diplom-ingenieur degree in electronics from the University of Stuttgart, Germany, in 1981.

He worked for Dornier Systems GmbH from 1982 to 1985 as a development engineer for power converters in spacecraft applications. From 1986 to 1988 he worked as a research and development manager for industrial ac and dc power converters at Brandner KG in Germany. Since 1989 he has been director of Convertec Ltd. in Ireland. Convertec develops high-reliability power converters for industrial applications.